Three types of chaos in the forced nonlinear Schrödinger equation

Eli Shlizerman* and Vered Rom-Kedar†
Weizmann Institute of Science, Israel
(Dated: November 1, 2005)

Three different types of chaotic behavior and instabilities (homoclinic chaos, hyperbolic resonance and parabolic resonance) in Hamiltonian perturbations of the nonlinear Schrödinger (NLS) are described. The analysis is performed on a truncated model using a novel framework in which a hierarchy of bifurcations is constructed. Then, it is demonstrated numerically that the forced NLS equation exhibits analogous types of chaotic phenomena. The study reveals that an adjustment of the forcing frequency sets the behavior near the plane wave solution to one of the three different types of chaos for any periodic box length.

PACS numbers: 42.65.Sf, 45.20.Jj, 52.35.Mw, 05.45.-a

The one dimensional nonlinear Schrödinger equation emerges as a first order model in a variety of fields - from high intensity laser beam propagation to Bose-Einstein condensation to water waves theory. The NLS is completely integrable, hence solvable, in one dimension on the infinite line or with periodic boundary conditions. The realization that the integrable structure might not persist under small perturbations led to the investigation of the forced and damped NLS [1]. Extensive numerical studies of this equation and of its two mode Galerkin truncation showed that indeed the perturbation gives rise to rich and complicated dynamics and that the finite dimensional model faithfully mimics the PDE dynamics when even and periodic boundary conditions are imposed and the L_2 norm of the initial data is not too large [2, 3], see also [4] for a similar behavior in a nonlocally coupled NLS system. In this letter we provide a new classification of chaotic orbits in the perturbed, undamped two-mode model, and reveal a new type of chaotic behavior: parabolic resonance. Moreover, we suggest that in some phase-space regimes there exists an analogous classification of the chaotic behavior of the forced NLS.

Consider the forced NLS equation (with no damping):

$$-i\psi_t + \psi_{xx} + |\psi|^2\psi = i\varepsilon \exp(-i\Omega^2 t), \qquad (1)$$

with periodic boundary conditions and with even solutions in x: $\psi(x,t) = \psi(x+L,t) = \psi(-x,t)$. Let $B = \psi \exp(i\Omega^2 t)$. B satisfies the same boundary conditions as ψ and the autonomous equation:

$$-iB_t + B_{xx} + (|B|^2 - \Omega^2)B = i\varepsilon. \qquad (2)$$

In this context, the perturbed NLS was first derived as a small amplitude envelope approximation of the damped driven Sine-Gordon Equation when the driving force is near resonant [2, 5]; then Ω is set to $\Omega = 1$ and the only parameter appearing in the unperturbed system is the period L. Here we show that it is possible to tune the system into different types of chaos by varying Ω and keeping L fixed.

For $\varepsilon = 0$ Eq. (2) possesses infinite number of constants of motion. The first two are the "particle number" $\mathcal{I} = \int |B|^2 \,\mathrm{dx}$ and the "energy" $\mathcal{H}_0 = \int \left(-|B_x|^2 + \frac{1}{2}|B|^4 - \Omega^2|B|^2\right) \,\mathrm{dx}$. The total energy $\mathcal{H}_0 + \varepsilon\mathcal{H}_1$ is also preserved when adding the perturbation $\mathcal{H}_1 = i\int (B - B^*) \,\mathrm{dx}$. Since the forcing term is x independent, the space of spatially uniform solutions ($B(x,t) = \frac{1}{\sqrt{2}}c(t)$) is invariant under the perturbed flow (2). In the unperturbed system these are the plane waves solutions, which are time periodic and are of the form $c(t) = |c(0)|\exp[i\gamma(t)] = |c(0)|\exp[i(\Omega^2 - \frac{1}{2}|c(0)|^2)t + i\gamma(0)]$, so γ is the phase of the plane wave. More generally, we define $c(t)$ to be the (complex) spatial average of a solution, $c(t) = \sqrt{2}\left\langle B(x,t)\right\rangle_x$, and γ to be the argument of this average, $\gamma(t) = \arg\left\langle B(x,t)\right\rangle_x$. Then, the plane waves appear as circles in the complex c plane, with periodic motion along these circles whenever $\Omega^2 \neq \frac{1}{2}|c(0)|^2$. When $\Omega^2 = \frac{1}{2}|c(0)|^2$ (so $\dot\gamma = 0$) the periodic motion along the plane wave and the forcing period are in *resonance*.

Linear stability analysis or "Modulation Stability" of the plane waves at $\varepsilon = 0$, shows that the solution is stable (*elliptic*) when $|c(0)| < \frac{2\pi}{L}$, neutral (*parabolic*) when $|c(0)| = \frac{2\pi}{L}$ and unstable (*hyperbolic*) with exactly one unstable linear mode, $\cos\frac{2\pi}{L}x$, when $\frac{2\pi}{L} < |c(0)| \leq \frac{4\pi}{L}$. *We propose that the behavior of the perturbed solutions near the plane wave depends primarily on its local stability* ***and*** *on the rotation rate on it ($\dot\gamma$).*

To demonstrate our approach on the NLS system, we follow [6–8], and study first a two-mode Galerkin truncation of the forced NLS:

$$B_2(x,t) = \frac{1}{\sqrt{2}}c(t) + b(t)\cos(kx), \qquad (3)$$

where the periodic boundary conditions imply that $k = \frac{2\pi}{L}j$, $j \in Z_+$, so for the first unstable mode $k = \frac{2\pi}{L}$. Substituting this solution in the forced NLS equation (2), and neglecting (see [1–3, 5] for discussion of this step) higher Fourier modes, a two degrees of freedom near integrable Hamiltonian system is found:

$$H(c,c^*,b,b^*;\varepsilon) = H_0(c,c^*,b,b^*) + \varepsilon H_1(c,c^*,b,b^*), \quad (4)$$

*Electronic address: eli.shlizerman@weizmann.ac.il
†Electronic address: vered.rom-kedar@weizmann.ac.il

with the Poisson brackets $\{\cdot,\cdot\} = -2i\left\langle \frac{\partial}{\partial c}, \frac{\partial}{\partial c^*} \right\rangle - 2i\left\langle \frac{\partial}{\partial b}, \frac{\partial}{\partial b^*} \right\rangle$, where

$$\begin{aligned} H_0 &= \frac{1}{8}|c|^4 + \frac{1}{2}|b|^2|c|^2 + \frac{3}{16}|b|^4 - \frac{1}{2}(\Omega^2+k^2)|b|^2 \\ &\quad - \frac{\Omega^2}{2}|c|^2 + \frac{1}{8}(b^2c^{*2} + b^{*2}c^2), \qquad (5) \\ H_1 &= \frac{i}{\sqrt{2}}(c - c^*). \end{aligned}$$

At $\varepsilon = 0$, these equations are integrable and possess an additional integral of motion, $I = \frac{1}{2}(|c|^2 + |b|^2)$, see [3]. A remarkable property of this truncation is that the two integrals of motion of the truncated model correspond to the first two invariants of the unforced PDE. Furthermore, the spatial independent solutions of the NLS correspond to the invariant plane $(c, b) = (|c(0)| \exp[i\gamma(t)], 0)$ of the truncated model. When the plane wave becomes unstable, both the PDE and the ODE systems possess homoclinic orbits structure - there exist solutions which are asymptotic to the plane wave solution as $t \to \pm\infty$ [9].

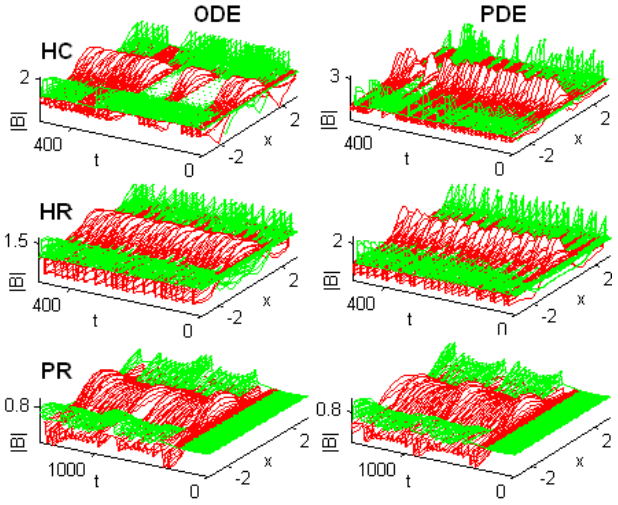

FIG. 1: (Color online) The amplitude plot - $|B(x,t)|$ vs. (x,t). We color the centered profiles ($x = 0$) by black(red) and the winged ones ($x = \pm L/2$) by light gray(green) (according to the spatial position of the maximum of $|B(x,t)|$). In all figures: $k = 1.025$ and $\epsilon = 10^{-4}$ and the initial conditions are: $B(0) = (I_{init} + 10^{-5}(1+i)\cos kx)e^{i\pi/4}$, where the labels indicate: HC-homoclinic chaos ($\Omega = 1, I_{init} = \sqrt{3/2}$), HR-hyperbolic resonance ($\Omega = I_{init} = 1$), PR-parabolic resonance ($\Omega = \frac{1.025}{\sqrt{2}}, I_{init} = 0.5125$).

The investigation of this truncated system when the plane wave is unstable and in resonance led, a decade ago, to the discovery of a new mechanism of instability - the hyperbolic resonance [6–8]. New methodologies and tools introduced to this PDE-ODE study have finally led to a proof that the homoclinic resonance dynamics, and in particular the birth of new types of multi-pulse homoclinic orbits which is associated with it, has analogous

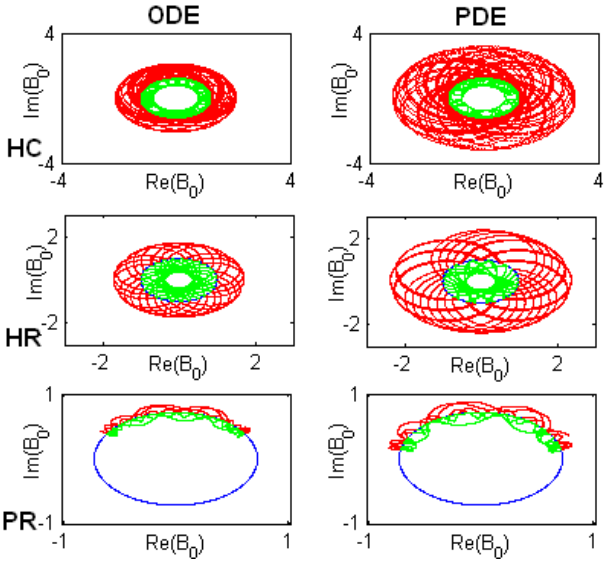

FIG. 2: (Color online) B-plane plot - $B(x,t)|_{x=0}$ in the complex plane. Black(Blue) circle correspond to initial plane wave solution.

behavior in the PDE setting (see [3, 10, 11] and references therein). Here, we propose that more generally, to classify the behavior near the plane waves one needs to consider both its local stability and its rotation rate, and in particular, we propose that when the plane wave is parabolic and in resonance, new type of solutions appear.

To fully classify the perturbed motion in the truncated model we introduced in [12, 13] the general framework of "hierarchy of bifurcations" and used it to analyze the integrable structure. The main tools in this framework are the *energy-momentum bifurcation diagrams* (EMBD) and the Fomenko graphs. These give a succinct representation to the structure of the energy surfaces; the structure of the level sets on a given surface (H_0 is fixed and I is varied) is described by Fomenko graphs (the first level of the hierarchy). Changes in the energy surfaces structure as the energy is varied is described by the EMBD (second level) and changes in these diagrams as parameters are varied are described by the critical energies bifurcation diagram and correspond to the third level of the hierarchy. Performing this analysis for the truncated model (see [12]), we obtained the following classification of the solutions; For most values of $(c(0), b(0))$, and in particular near the plane wave solutions ($b = 0$) with $I^{pw} < \frac{1}{2}k^2$ where they are normally elliptic, the solutions of the unperturbed systems are quasi-periodic. Hence, under perturbation, most of these quasi-periodic motions persist (by KAM theory) and small resonance zones appear as well. Due to the nonlinearity, and the fact that this is a two-degrees of freedom system, for sufficiently small perturbations the perturbed motion always stays close to the unperturbed plane wave circle.

For $I^{pw} > \frac{1}{2}k^2$ the plane wave is normally hyperbolic - a figure eight homoclinic loop is created. If $I^{pw} \neq \Omega^2$,

unperturbed homoclinic solutions have a non-zero spatial average which oscillates in time and a spatial term which is centered at either $x = 0$ ("central configuration") or $x = \frac{L}{2}$ ("wing configuration") and decays, as $t \to \pm\infty$, to zero. For the unperturbed system, on the same energy surface, two normally stable periodic solutions are created. These solutions are of the form $(c, b) = (|c(0)|, \pm|b(0)|)\exp(i\gamma(t))$ - the plus sign corresponds to a central solution whereas the minus sign corresponds to a winged solution (the even boundary conditions lead to this selection of relative equilibria). Thus, on this energy surface, if $\frac{1}{2}k^2 > \Omega^2$, unperturbed orbits with initial conditions near the plane wave with $I > I^{pw}$ encircle the figure eight, jumping periodically from central to winged configuration. Solutions with $I < I^{pw}$ oscillate around the stable periodic orbits, having either central or winged configuration.

We propose that for particle numbers $I < 2k^2$, near the plane wave solutions, the above qualitative description of the truncated system applies to the forced NLS as well, where $c(t)$ represents the spatial average of $B(x,t)$ and $b(t)$ represents the complex amplitude of the leading (e.g. most energetic) spatial dependent mode of the solution: $B(x,t) = c(t) + b(t)\phi_1(x) + ...$ For small particle numbers ($I(0) < \frac{1}{2}k^2$), most solutions starting near the plane wave exhibit quasi-periodic motion in time, where one of its frequencies is associated with γ and the other one with the spatial oscillations around the spatial mean. The spatial center of these solutions moves periodically from the central to the wing configuration and back. When the plane wave becomes hyperbolic, spatial excitations which are periodic in time are created - these are the PDE analogs to the two periodic solutions of the truncated model with non-zero b. These solutions are the spatially-periodic "solitons" appearing, because of the even boundary condition, in central or wing configuration. The figure eight orbits of the truncated model correspond to the NLS asymptotic solutions in time - the homoclinic orbits to the plane wave solution $B_h \overrightarrow{_{t\to\pm\infty}} B_{pw}$.

The perturbed solutions near the hyperbolic plane wave exhibit homoclinic chaos; a chaotic zone is created near the unperturbed separatrices and the solutions change their spatial center chaotically in time, as demonstrated in Fig. 1 (in the ODE column of the figures we use equation (3) to reconstruct $B(x,t)$ from the two-mode model). This chaotic zone is essentially uniform in the γ variable (different sections in γ are topologically conjugate) as demonstrated in Figs. 2 and 4, since for almost all Ω values the motion rate does not vanish ($|\dot{\gamma}| > 0$). We refer to this behavior as *homoclinic chaos*.

The uniformity of the perturbed solutions in the phase is lost when $\dot{\gamma}$ vanishes in the unperturbed system, namely when $I = I_r^{pw} = \Omega^2$. Then, for $\frac{1}{2}k^2 < \Omega^2$ (so $I_r^{pw} > \frac{1}{2}k^2$) a *hyperbolic resonance* appears [6–8], see Figs. 2 and 4. Notice that when $\Omega = 1$ only small wave numbers ($k < \sqrt{2}$) satisfy this condition. By introducing the additional parameter Ω we find that *for any k value there is an interval of Ω values for which the resonant plane wave circle is hyperbolic*: it is hyperbolic for all $\Omega > \frac{1}{\sqrt{2}}k$.

Finally, we observe that the plane wave is normally parabolic when $I = I_p^{pw} = \frac{1}{2}k^2$. For most Ω values the perturbed motion near the parabolic plane wave remains close to it just as in the elliptic case, since the separatrix is small and its splitting is exponentially small in the distance from the bifurcation point. However, when it is parabolic and resonant (so $I = I_r^{pw} = I_p^{pw}$, namely $\Omega = \Omega_{pr} = \frac{1}{\sqrt{2}}k$), the situation is dramatically changed as is demonstrated in all the figures of this letter (see also [14][12, 13]). In particular, initial conditions near the parabolic plane wave do not stay close to it. It follows from [12] that the above list exhausts all types of dynamical phenomenon which may exist in the truncated model near the plane wave solution for finite k and Ω, for $I < 2k^2$.

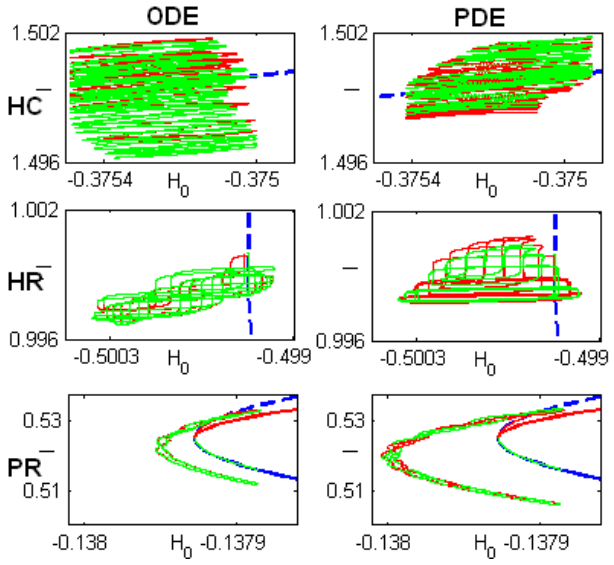

FIG. 3: (Color online) EMBD diagram. $I(t)$ - particle number, $H_0(t)$ - instantaneous unperturbed energy. Gray(Blue) curve - (I, H_0) on the plane waves. Black(Red) curve - (I, H_0) on the periodic spatial solitons. Solid-stable. Dashed-unstable.

With this interpretation we can now examine the behavior of the forced NLS near the plane wave in the three situations of interest: the hyperbolic chaos case (HC), the hyperbolic resonance case (HR) and the parabolic resonance case (PR). Indeed, with the above analysis it is clear how to initialize the simulations to obtain each of these behaviors. In all cases we choose to start with a small perturbation from the plane wave (small $|b(0)|$); to obtain the HC situation we choose for any (Ω, k) any $I(0) \in (\frac{1}{2}k^2, 2k^2)$ which is bounded away from Ω^2. To obtain HR, we take $I(0) \approx \Omega^2$ and $\frac{1}{2}k^2 < \Omega^2$, whereas PR is observed when $\frac{1}{2}k^2 \approx \Omega^2$ and $I(0) \approx \Omega^2$. In the simulations we set $k_{init} = 1.025$ (as in [2, 5]) and set $\Omega^2_{init} = 1$ in the HR and HC cases and take

$\Omega^2_{init} = \frac{(k_{init})^2}{2}$ in the PR case. The ODE simulations were computed with a standard ODE solver and we verified that the largest Lyapunov exponents of the three solutions are positive and thus they are indeed chaotic. The PDE simulations were computed with a scheme of 4th order Runge-Kutta in time and 8th order central differences in space. We verified that the total energy is well conserved ($|\mathcal{H}_0(t)+\varepsilon\mathcal{H}_1(t)-\mathcal{H}_0(0)-\varepsilon\mathcal{H}_1(0)| < 10^{-5}$) and that the numerical simulations in [15] are reproduced.

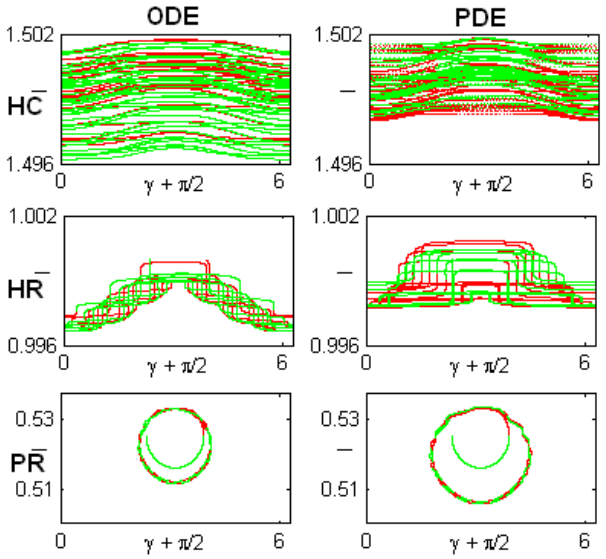

FIG. 4: (Color online) Action-angle diagram - γ vs. I.

In Fig. 1 we present $|B(x,t)|$ as a function of (x,t) for a small interval of time - the chaotic hopping between central and wing configuration is well observed, as is the similarity between the truncated and the full model. Furthermore, the strong modulation in the maximal amplitude of the PR solutions clearly distinguishes it from the HC and HR cases. We also observe that the parabolic resonance solution has two regions - almost periodic and chaotic. In Fig. 2 we plot, similarly to [3, 15], $(\mathrm{Re}\{B(0,t)\}, \mathrm{Im}\{B(0,t)\})$ for some interval t. For reference, we plot in gray(blue) the circle corresponding to the plane wave which has the same energy (H_0) as the chosen initial conditions. The strong non-uniformity in the phase of the parabolic resonant solutions is apparent in the truncated and the full models alike.

In Fig. 3 a new presentation of the solutions is proposed - the motion in the space of the unperturbed invariants (H_0 and I) is presented, so that the phase information is filtered out. In addition, the underlying integrable backbone, which comprises the EMBD is shown; The values of (H_0, I) at the periodic solutions are presented as curves in the plot. The gray(blue) curve corresponds to the plane wave solution and the black(red) curve to the two periodic spatial profiles, dashed when they are unstable and solid when they are stable. The different signatures of the HC, HR and PR are clearly seen, as are the long quasi-integrable segments of the PR solutions.

Finally, to elucidate the different role which is played by the phase of the spatial average of B, we present the "action-angle" diagram of (γ, I) (Fig. 4). We observe that the main difference between the regular homoclinic chaos and the hyperbolic resonant chaotic motion has to do with the non-uniformity in the γ variable - thus it is not observable in the amplitude plot. Furthermore, Figs. 3-4 direct us to a possible description of parabolic resonance. Notice the paths of the trajectory in the EMBD plot which strongly suggest that adiabatic description of some segments of the motion is appropriate. It appears that the action in the normal plane is a key ingredient in understanding the perturbed motion as it is adiabatically preserved [16].

Summarizing, the numerical results suggest that near the plane waves, for particle numbers which are smaller than $2k^2$, there are three types of chaotic instabilities which are well captured by the two mode model. Furthermore, parabolic resonances, which correspond to a new type of chaotic behavior, were shown to exist in the forced NLS model and lead to a large variation in the particle number of the solution.

We acknowledge the support of the Israel Science Foundation (Grant 926/04) and the Minerva foundation.

[1] A. R. Bishop and P. S. Lomdahl, Phys. D **18**, 54 (1986).
[2] A. Bishop, R. Flesch, M. Forest, D. McLaughlin, and E. Overman II, SIAM J. Math. Anal. **21**, 1511 (1990).
[3] D. Cai, D. W. McLaughlin, and K. T. R. McLaughlin, in *Handbook of dynamical systems, Vol. 2* (North-Holland, Amsterdam, 2002), pp. 599–675.
[4] M. Higuera, J. Porter, and E. Knobloch, Phys. D **162**, 155 (2002).
[5] A. Bishop, M. Forest, D. McLaughlin, and E. Overman II, Physics Letters A **144**, 17 (1990).
[6] G. Kovacic and S. Wiggins, Physica D **57**, 185 (1992).
[7] G.Kovacic, J. Dynamics Diff. Eqns. 5 pp. 559–597 (1993).
[8] G. Haller and S. Wiggins, Physica D **85**, 311 (1995).
[9] N. Ercolani, M. G. Forest, and D. W. McLaughlin, Phys. D **43**, 349 (1990).
[10] G. Haller, *Chaos Near Resonance*, Applied Mathematical Sciences; 138 (Springer-Verlag, NY, 1999).
[11] D. W. McLaughlin and J. Shatah, in *Recent advances in partial differential equations* (Amer. Math. Soc., Providence, RI, 1998), vol. 54, pp. 281–299.
[12] E. Shlizerman and V. Rom-Kedar, Chaos **15** (2005).
[13] A. Litvak-Hinenzon and V. Rom-Kedar, SIAM J. Appl. Dyn. Syst. **3** (2004).
[14] V. Rom-Kedar, Chaos **7**, 148 (1997).
[15] D. W. McLaughlin and E. A. Overman, II (Plenum, NY, 1995), vol. 1, pp. 83–203.
[16] A. I. Neishtadt, Prikl. Mat. Meh. **39**, 1331 (1975).